Compact energy dispersive X-ray microdiffractometer for diagnosis of neoplastic tissues

C. Sosa[a,b], A. Malezan[c], M.E. Poletti[c,*], R.D. Perez[a,b,**]

[a] Universidad Nacional de Córdoba, Ciudad Universitaria, Córdoba, Argentina
[b] Consejo Nacional de Investigaciones Científicas y Técnicas-CONICET, Buenos Aires, Argentina
[c] Departamento de Física da Faculdade de Filosofia, Ciências e Letras de Ribeirão Preto. Universidade de São Paulo, Brazil

ARTICLE INFO

ABSTRACT

An energy dispersive X-ray microdiffractometer with capillary optics has been developed for characterizing breast cancer. The employment of low divergence capillary optics helps to reduce the setup size to a few centimeters, while providing a lateral spatial resolution of 100 µm. The system angular calibration and momentum transfer resolution were assessed by a detailed study of a polycrystalline reference material. The performance of the system was tested by means of the analysis of tissue-equivalent samples previously characterized by conventional X-ray diffraction. In addition, a simplified correction model for an appropriate comparison of the diffraction spectra was developed and validated. Finally, the system was employed to evaluate normal and neoplastic human breast samples, in order to determine their X-ray scatter signatures. The initial results indicate that the use of this compact energy dispersive X-ray microdiffractometer combined with a simplified correction procedure is able to provide additional information to breast cancer diagnosis.

1. Introduction

X-ray diffraction (XRD) and medical imaging techniques can be successfully combined to provide a powerful tool able to differentiate tissues with similar X-ray attenuation characteristics (Kosanetzky et al., 1987; Speller, 1999; Bradley and Wells, 2013; Harding and Schreiber, 1999). XRD analysis discriminates between glandular, adipose and neoplastic breast tissues becoming a helpful tool for breast cancer diagnosis (Speller, 1999; Kidane et al., 1999; Poletti et al., 2002a, 2002b; Cunha et al., 2006; Griffiths et al., 2007; Ryan and Farquharson, 2007; Oliveira et al., 2008; Pani et al., 2010). For this application, the Energy Dispersive X-Ray Diffraction (EDXRD) technique is useful to reduce the acquisition time and simplify the detection system (Clark, 2002). These advantages are consequence of employing a solid state detector with high energy resolution, which performs simultaneous energy scanning of the scattered beam, avoiding complex mechanical motions.

In an energy dispersive configuration, a polychromatic excitation beam with low divergence is required to apply the Bragg Law. Usually, it is obtained by means of the alignment of two small collimators with a large distance between them, in the order of several tens of centimeters (Kidane et al., 1999; Cunha et al., 2006; Ryan and Farquharson, 2007;

Pani et al., 2010; LeClair et al., 2006; King and Johns, 2010; Chaparian et al., 2010; King et al., 2011; Abdelkader et al., 2012; Tang et al., 2014a, 2014b). In the present work, we showed that the employment of capillary optics in the excitation channel reduces this distance to a few centimeters, giving rise to a compact setup. In addition, the lens also reduces the excitation area, keeping a high photon flux over the sample, which allows X-ray microdiffraction analysis (micro-XRD).

2. EDXRD methodology

2.1. Basic principles

An energy dispersive micro-XRD (micro-EDXRD) system combines the EDXRD with the spatial resolution of the X-ray microanalysis. EDXRD is a well-known method, which can be implemented without complex mechanical detector or source motion, since the scattering angle is fixed. It takes advantage of the high energy resolution semiconductor X-ray detectors technology to electronically scan the scattered beam, looking for constructive interference peaks. In the case of crystals, these peaks originate from coherent scattering at different atomic planes, according to Bragg's condition:

** Corresponding author at: Universidad Nacional de Córdoba, Ciudad Universitaria, Córdoba, Argentina.
* Corresponding author at: Departamento de Física da Faculdade de Filosofia, Ciências e Letras de Ribeirão Preto. Universidade de São Paulo, Brazil.
E-mail addresses: poletti@ffclrp.usp.br (M.E. Poletti), danperez@famaf.unc.edu.ar (R.D. Perez).

C. Sosa et al.

$$d = \frac{0.6199}{E\sin\theta} = \frac{1}{2x} \tag{1}$$

where d is the interplanar spacing of the lattice planes in nanometers (nm), 2θ is the scattering angle, E is energy of the scattered photon in keV and x is the momentum transfer, $x(nm^{-1})=[E(keV)/1.2398]\sin(\theta)$. Thus, the energy of any particular diffraction peak depends upon the scattering angle. In particular, this angle is adjusted such that the diffraction peaks of interest fall in the useful range of X-ray flux available from the used source (Clark, 2002). The Full Width at Half Maximum (FWHM) of a diffraction peak (ΔE_{FWHM}) depends upon the angular resolution of the system ($\Delta\theta$) and the energy resolution of the detector (ΔE_D). For a single peak, the ΔE_{FWHM} can be taken as the minimum energy separation between two resolved diffraction peaks, i.e., as a measure of the system to resolve the peaks in the momentum transfer space (momentum transfer resolution, $\Delta x/x$).

The D-spacing resolution ($\Delta d/d=\Delta x/x$) can be estimated from $\Delta\theta$ and ΔE_D by means of statistical error propagation derived from the Eq. (1):

$$\left(\frac{\Delta d}{d}\right)^2 = (\Delta\theta ctg\theta)^2 + \left(\frac{\Delta E_D}{E}\right)^2 \tag{2}$$

Considering that a high energy resolution detector (HPGe, Si(Li) or SDD) is chosen for the system configuration, the improvement of the momentum transfer resolution mainly depends on the effectiveness of the strategies to reduce the angular divergence of the system, $\Delta\theta$. The latter is related to the divergences of incident and scattered beams. The employment of a focusing lens with low divergence reduces the incidence divergence. In addition, the small transversal section of the focalized incident beam combined with thin sample thickness allow a reduction of the target volume (range of scattered angles) keeping the sample-detector distance in the range of few centimeters.

2.2. The energy spectrum of the scattered X-ray photons

The energy distribution of the number of detected scattered photons, $N(E)$, has contributions from many background sources (air, sample holder and collimators) and includes single and multiple scattering within the sample. In this work, the multiple scattering is neglected, because sample dimensions were small compared to the mean free path of the scattered photons (Kidane et al., 1999). The background spectrum (all contributions), $N^B(E)$, was measured (in the absence of the sample, but remaining all other scatter conditions the same) and subtracted from the detected scattering X-ray spectra, weighting by the transmission factor of the sample (Geraldelli et al., 2013):

$$N^{corr}(E) = N(E) - N^B(E)e^{-\mu(E)t} \tag{3}$$

where $\mu(E)$ and t are the linear attenuation coefficient and thickness of the sample, respectively. Therefore, it is possible to assume that the corrected spectrum, $N^{corr}(E)$, is related solely to single scattering events at the sample and can be approximated as (Geraldelli et al., 2013):

$$N^{corr}(E) = \varepsilon(E)N_o(E)\eta\frac{d\sigma}{d\Omega}(E)\Omega_D G_T(E) \tag{4}$$

where $\varepsilon(E)$ is the detector efficiency at energy E, $N_o(E)$ is the number of photons incident on the sample, η is the number of atoms or molecules per unit of volume, $d\sigma/d\Omega(E)$ is the differential total scattering cross section of an atom or molecule, Ω_D is the solid angle subtended by the detector and $G_T(E)$ is an appropriate geometric transmission factor (which accounts for both sample self-attenuation and geometry). For the EDXRD setup, a fixed position for the X-ray detector was selected in order to define the scattering angle 2θ. Then, all the factors in the previous equation show variations only with the incident energy. In addition, the values adopted for 2θ are usually of a few degrees in order

to neglect the energy variations produced by the incoherent scattering contribution (Clark, 2002). Thus, the differential total scattering cross section can be evaluated as $d\sigma/d\Omega(E)=[F^2(x)+F_{KN}.S(x)]d\sigma_{Th}/d\Omega$, where $d\sigma_{Th}/d\Omega$ is the Thomson differential cross section equal to $(r_o^2/2)(1+\cos^2 2\theta)$, r_o is the classical electron radius, $F(x)$ is the atomic or molecular structural form factor, F_{KN} is the Klein-Nishina function and $S(x)$ in the incoherent scattering function. In the case of biological tissues, the form factor profile depends on intramolecular as well as intermolecular interference effects, giving rise to particular diffraction patterns for each tissue. On the other hand, the Compton contribution to the differential total scattering cross section is often ignored because it is small and structureless over the measured momentum transfer range (Geraldelli et al., 2013).

The geometric transmission factor, $G_T(E)$, can be calculated by:

$$G_T(E) = e^{-\mu(E)t/\cos 2\theta}\left[\frac{e^{[(1/\cos 2\theta)-1]\mu(E)t}-1}{(1/\cos 2\theta - 1)\mu(E)}\right] \cong e^{-\mu(E)t/\cos 2\theta}t \tag{5}$$

The approximation equation is valid when the thickness is at least one order of magnitude smaller than the mean free path or for small angles such in our case.

3. Materials and methods

3.1. Instrumentation

The schematic diagram of the energy dispersive micro-XRD in transmission geometry employed in this work is shown in Fig. 1. The source was an W X-ray tube Philips model PW2275/20 operating at 60 kV–30 mA. The W anode was tilted 6° from the horizontal plane with focus dimension of 0.4 mm×12 mm, but it was oriented as to obtain a point source (0.4 mm×1.2 mm). Attached at the selected output, there was a high quality conical monocapillary made of borosilicate glass by drawing at high temperature in a heating furnace (Perez et al., 2008). Its inner diameter linearly decreases from 0.77 to 0.1 mm along 100 mm of length, providing an output divergence of 5 mrad. The lens was designed to produce a mean gain factor of 2 with a focal spot size of 100 μm at 3 mm of the tip. The wall of the lens was thick enough for an effective attenuation of the high energy X-ray photons. Radiation transport simulations were performed using a developed MATLAB® (MathWorks, USA) routine, which allows studying the energy dependence of transmission, divergence and focal size of the lens (Sosa et al., 2015).

The samples were placed 3 mm from the output of the lens. The diffraction angle 2θ was chosen as 7° in order to interrogate a momentum transfer region from 0.7 nm^{-1} to 2.5 nm^{-1}. This region corresponds to the range where most biological tissues exhibit interference effects (Speller, 1999; Kidane et al., 1999).

The scattered photons were collected by a SDD detector AMPTEK®. The distance from the entrance window of the detector and the surface sample was 70 mm. A 1 mm lead collimator delimited the acceptance angle of the detector. Acquisition time of 600 s was used to achieve appropriate statistical counting (i.e., uncertainties in the photon count smaller than 3% in the scattered energy spectra). The energy calibra-
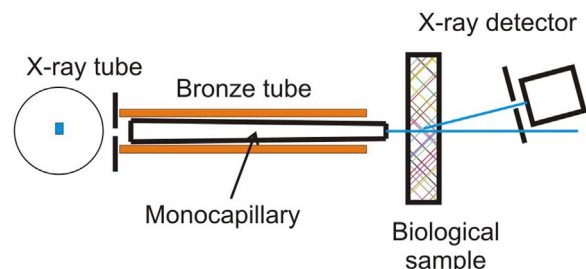

Fig. 1. Schematic diagram of the micro-EDXRD spectrometer presented in this work.